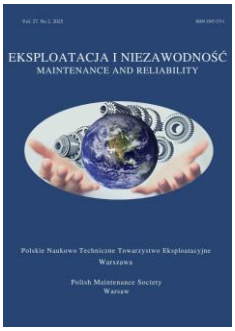

EksploatacjaiNiezawodnosc – Maintenance and Reliability
Volume 27 (2025), Issue 2
journal homepage: http://www.ein.org.pl

Article citation info:
Song S, Yang G, Cao C, Ma W, Fault Diagnosis Model of Hydraulic Motor Based on Fuzzy Neural Network, EksploatacjaiNiezawodnosc – Maintenance and Reliability 2025: 27(2) http://doi.org/10.17531/ein/195532

Fault Diagnosis Model of Hydraulic Motor Based on Fuzzy Neural Network

Indexed by:
Web of Science Group

Shoupeng Song[a,*], Guolai Yang[a], Chuanchuan Cao[a], Wei Ma[a]

[a]Energy and Power Engineering, Lanzhou University of Technology, China

Highlights

- Fuzzy neural network is used to predict hydraulic motor faults.
- The feature vector is output in the global mean pooling layer.
- The dynamic cluster graph is obtained by fuzzy clustering.

Abstract

When the hydraulic motor fault occurs, it is not easy to be detected, and the leakage degree will gradually increase. In order to avoid bigger accidents caused by the hydraulic motor fault, the accident is excluded in the embryonic stage, and the hydraulic motor fault prediction method based on fuzzy neural network is used to predict the hydraulic motor fault. The feature vector is output in the global mean pooling layer, and the feature vector matrix between the health state feature vector library and the samples to be measured is constructed. The dynamic cluster graph is obtained by fuzzy clustering, so as to realize the fault diagnosis of the hydraulic motor. The results show that the accuracy of training set, verification set and test set is higher than 99.8%. The accuracy of diagnosis classification is 99.00%, which is better than other comparison models. In this study, the number of training samples can be appropriately increased or decreased according to the curve complexity of the detection target, so as to improve the feature extraction capability of the convolutional layer and increase the classification accuracy.

Keywords
convolutional neural network, clustering, fuzzy neural network, fuzzy control, fuzzy logic, hydraulic motor

1. Introduction

Hydraulic motor is the key power component of hydraulic system. Once an internal leakage fault occurs, it is difficult to accurately diagnose the cause of the fault without certain experience and fault diagnosis technology [1]. Therefore, for the failure caused by the leakage of the hydraulic system, the maintenance personnel can only blindly disassemble the hydraulic system if they cannot determine the cause of the fault, and even cause deformation or damage to the parts in the blind disassembly process, resulting in greater economic losses. The application of transfer learning and continuous learning in hydraulic motor fault diagnosis mainly involves using existing knowledge and data to solve new problems and improve the accuracy and efficiency of fault diagnosis. Transfer learning transforms and aligns the features extracted under different processes through domain adaptive methods, so that the process distributions of source domain and target domain are similar, thus improving the model's diagnostic capability in target domain [2]. Faced with the problem of reduced fault identification accuracy and small sample size caused by motor parameter changes, continuous learning can help the model adapt to these changes [3]. However, to make the prediction results more accurate for the existing model, it

(*) Corresponding author.
E-mail addresses: S. Song (ORCID: 0009-0009-5555-6413) ssp4346@sina.com, G. Yang (ORCID: 0009-0009-7995-7887) xuexi1019@163.com, C. Cao (ORCID: 0009-0002-2233-782X) jiayouchong888@126.com, W. Ma (ORCID: 0009-0008-3464-4302) kaixinggogogo@sina.com

is necessary to build a good model or have enough experience [4]. Transfer learning and continuous learning can predict the state of a device with enough data. However, the difference between healthy and sub-healthy states was small. There are few data about sub-health and faults, which cannot meet the parameter training requirements of general diagnostic models and the difficulty of sub-health identification [5-6]. In this paper, the advantages of fuzzy recognition that can complete classification without training and convolutional neural network (CNN) that can extract tiny features are used to collect the performance parameters of hydraulic system under the condition of hydraulic motor leakage fault, which provides data support for fault prediction research. Finally, based on fuzzy clustering, fuzzy logic theory and improved residual network, the hydraulic motor fault prediction and diagnosis model is constructed, and the hydraulic motor fault diagnosis and prediction can be completed with only a few data samples.

The novelty of this research is shown as follows: (1) The fault prediction model based on T-S fuzzy neural network is established by using fuzzy model recognition algorithm. The fault diagnosis is realized. (2) The feature vector standard model library is established, which can complete the classification without data training, solving the less training data. It has strong adaptability and small sample size. (3) Global Average Pooling (GAP) layer is used to replace the fully connected network in improved residual network (Resnet). The fuzzy clustering is used to replace the classification layer of the Resnet. A small amount of data is used to train the parameters of GAP layer, which improves the feature extraction ability of the model. (4) The fully connected layer and classification layer are improved. The classification accuracy is increased by appropriately adding training samples.

The contributions of this research are shown as follows: (1) The fault diagnosis of hydraulic motor can be completed without data training, which solves the less training data. It has strong adaptability and small sample size. (2) The performance monitoring and fault warning of hydraulic motors have been completed, saving maintenance resources and reducing lifecycle costs. They can also be used for fault research of other hydraulic components.

The research is divided into four parts in total. The first part analyzes the current research on hydraulic motor fault prediction and diagnosis. The second part constructs a fault prediction and diagnosis model for hydraulic motors. The third part is to verify the performance of the predictive diagnostic model. The fourth part summarize the research.

2. Related Works

Information technology and artificial intelligence technology have driven the development of intelligent and advanced hydraulic motor fault prediction and diagnosis. In recent years, scholars at home and abroad have conducted extensive research on the working principle and fault prediction and diagnosis methods of hydraulic pumps. However, research on fault prediction and diagnosis of hydraulic motors is scarce [7-9]. Aiming at the difficulty of extracting representative fault features from mixed vibration signals in industrial applications, Long et al. applied visual word package and pyramid histogram cross kernel support vector machine to complete fault diagnosis and state recognition of related motors, thus effectively improving the fault diagnosis accuracy [10]. Lu et al. proposed a heterogeneous computing framework. An integrated embedded system was designed, aiming at the problems related to processing off-line signals in motor fault diagnosis. It provides a solution for on-site motor fault diagnosis on small, flexible, and convenient handheld devices [11]. For the analysis and processing of bearing fault signals, Ke et al. optimized the white noise amplitude in the comprehensive empirical mode decomposition using the global optimality of genetic algorithm, thus providing data theoretical support for improving the accuracy of hydraulic motor fault prediction [12]. The motor fault diagnosis method is easily affected by different working conditions. Therefore, Long et al. obtained fault states through statistical analysis of matching points and dictionary templates generated by normal and abnormal motor signals. This solves the changes in machine operating conditions and improves the accuracy of fault diagnosis [13].

For complex systems, it is often difficult to correctly describe the dynamics of the system due to many variables. Dai et al. analyzed the main technologies used in intelligent fault diagnosis and the research status of hydraulic system fault diagnosis. The important application prospects of deep

learning in intelligent fault diagnosis were proposed. The main ideas, methods, and principles of several typical deep neural networks were described [14]. Sun et al. proposed a fault diagnosis method for asynchronous motors based on deep neural networks. It used sparse auto-encoders to learn features and added partial damage to the input to improve the robustness of feature representation. To prevent over-fitting during training, the regularization method dropout was adopted to achieve better results in feature learning and classification in the induction motor fault diagnosis [15]. Soni et al. adopted a new method combining fuzzy logic controller with fuzzy clustering method. The expert system combined with key parameters such as dissolved gas analysis, water content, interfacial tension and polymerization degree to diagnose and predict early faults of power transformers, providing basis for asset management decisions [16]. Soni et al. introduced a new adaptive neural fuzzy inference system model. This model was based on the moisture content, IFT, harmonics, and temperature rise data within the insulation layer to analyze the insulation degradation of oil and paper. The newly proposed model was validated using various real data collected from industries and literature, with an efficiency of over 90% and an error of less than 1% [17].

From the research of domestic and foreign scholars, the current methods for diagnosing hydraulic motor faults are difficult to meet practical requirements in small samples. However, model fault diagnosis technology overly relies on the digitization of diagnostic objects, making it difficult to establish accurate digital models in practical applications due to the complexity of diagnostic objects. In addition, model fault prediction technology hassome limitations in practical engineering applications. It is difficult to form a comprehensive expert knowledge base in practical work using knowledge based fault prediction techniques. Especially when new fault phenomena occur, it is hard for existing expert knowledge bases to find corresponding rules. There may even be situations where there is no expert knowledge base for similar fault phenomena. Meanwhile, no research on hydraulic motor fault experiments and intelligent prediction diagnosis methods has been found. There is no method to combine the two for analysis. Moreover, the corresponding relationship between various types of hydraulic motor faults and vibration signals has not been explored. The effective training sample library is relatively insufficient. Based on this, the hydraulic motor fault prediction and diagnosis model based on the fuzzy clustering, fuzzy logic theory, and improved residual network is innovative. It innovatively implements the full life cycle state evaluation and analysis of hydraulic motors in theory, and solves the enterprise hydraulic motor testing relying too much on human experience in practice. It lays the data and method foundation for promoting the intelligent prediction and diagnosis of hydraulic motor faults.

3. Full life cycle state assessment analysis of pre-fault prediction and post fault diagnosis for hydraulic motors

Currently, the troubleshooting hydraulic motors in important hydraulic systems on airplanes mainly focuses on fault prediction and diagnosis, without a combined analysis for the two. Therefore, this section mainly uses fuzzy logic theory and improved Resnet to achieve full life cycle state evaluation of hydraulic motors.

3.1. Pre-fault prediction and feature extraction analysis of hydraulic motors

Simply diagnosing faults in hydraulic motors cannot obtain complete accuracy. There are malfunctions that cannot be diagnosed. The actual analysis of research focuses on fault diagnosis. However, to achieve a more comprehensive fault diagnosis effect for hydraulic motors, the fault prediction is carried out before fault diagnosis to evaluate the full life cycle operation status of hydraulic motors. Generally speaking, the fault prediction method based on models is more accurate than the fault prediction method using knowledge and data. However, the data fault prediction only requires sufficient data to achieve the equipment status prediction through data analysis. Therefore, considering the actual experimental environment and subsequent fault diagnosis needs, a hydraulic motor fault prediction method based on data is studied. Among them, in intelligent technology, fuzzy theory can only provide uncertain descriptions in known information. The results obtained by fuzzy methods are much better than those obtained by traditional quantitative analysis. Therefore, the fuzzy inference model in fuzzy theory is chosen as the basic algorithm for predicting hydraulic motor faults [18-19].

The fuzzy reasoning model is proposed by Takagi and Sugeno, which is also known as the T-S model. For T-S type fuzzy systems, they are generally defined in the "if then" format. The fuzzy reasoning expression is shown in equation (1).

$$\begin{aligned} G^j: If\, p_1 is B_1^j, p_2 is B_2^j, \cdots, p_m is B_m^j \\ q_j = x_0^j + x_1^j p_1 + \cdots + x_m^j p_m \end{aligned} \quad (1)$$

In equation (1), G^j represents the rule. j is the number of fuzzy subsets, with a maximum value of o. p represents the input variable. B represents a fuzzy set. q represents the output variable. i represents the actual number of input parameters, with a maximum value of m. The membership, ambiguity, and output values of the input variables are expressed in equation (2).

When the known information can only be described with uncertainty, the results obtained by fuzzy methods are much better than those obtained by traditional quantitative analysis. The characteristics of phenomena usually described by fuzzy sets are relatively fuzzy. Fuzzy sets are a generalization of classical sets. A real number between 0 and 1 can be used to represent the membership degree, rather than just the 0 or 1 that represents membership in classical sets. Equation (2) represents any mapping μ_A from X to the closed interval [0,1].

$$\begin{cases} \mu_A: X \to [0,\ 1] \\ \mu \to \mu_A(\mu) \end{cases} \quad (2)$$

A is a fuzzy subset of X. μ_A is called the membership function of the fuzzy subset. $\mu_A(\mu)$ is called the membership degree of μ to A. When the membership function is used to represent a fuzzy description, its essence is to eliminate the fuzziness of the fuzzy description. When the object to be measured is determined, for each category in domain X, only the membership function of the category needs to be used to find the membership degree with the object to be measured. There are n fuzzy subsets on domain $X = (x_1,\ x_2, \cdots, x_n)$. A_1, A_2, ..., A_n, constitutes the standard data model library. For any $x_0 \in X$, $k \in \{1,\ 2, \cdots, n\}$ satisfies formula $A_k(x_0) = \vee \{A_1(x_0),\ A_2(x_0),\ \cdots,\ A_n(x_0)\}$. Then the x_0 is considered relative to A_k.

However, the T-S model is constructed based on fuzzy logic. Therefore, it lacks adaptive learning ability and requires massive manual operations in the logical reasoning, resulting in slow inference speed and relatively low accuracy [20-22]. Neural networks perform calculations through parallel connections between multiple neurons, resulting in high fault tolerance and strong self-learning ability. However, neural networks have high accuracy for the required input information, which also cannot explain the learning process for uncertain objects. It is not suitable for processing rule-based expert experience knowledge [23-24]. Therefore, the study combines the two and fully absorbs their advantages to construct a T-S fuzzy neural network model, as shown in Figure 1.

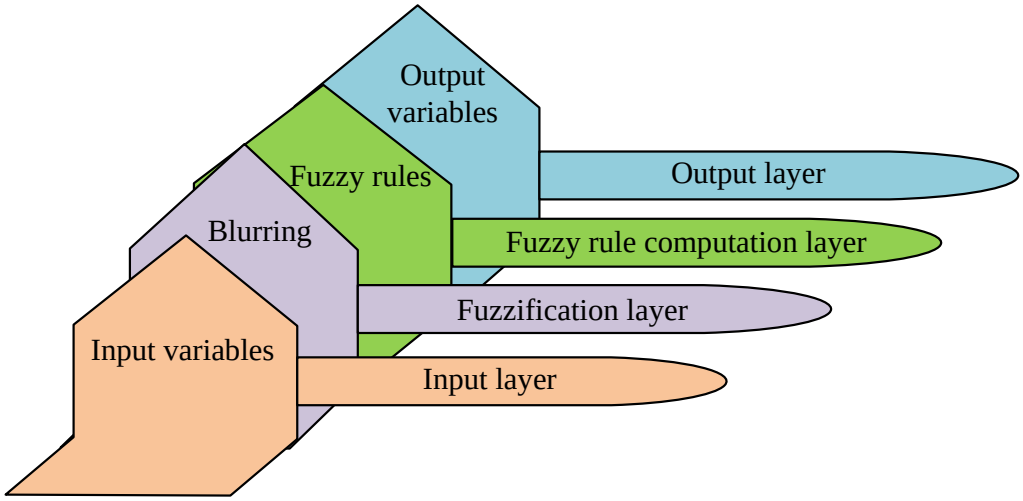

Figure 1. Schematic diagram of the hierarchical architecture of T-S fuzzy neural network model.

From Figure 1, the T-S fuzzy neural network model constructed in the study is divided into four levels, namely the input layer, blurring layer, fuzzy rule calculation layer, and output layer. The input layer passes the input variable $p = [p_1,\ p_2,\ \cdots,\ p_k]$ to the blurring layer. The number of input nodes inside it is equal to the number of dimensions of the

input variable. The fuzzy layer performs corresponding fuzzy processing on the actual values transmitted by the input layer. Specifically, the fuzzy membership value is obtained from equation (3).

$$\gamma_{\left(B_i^j\right)} = exp\left(-\frac{\left(p_i - a_i^j\right)^2}{d_i^j}\right),\ j = 1,\ 2,\ \ldots,\ k;\quad i = 1,\ 2,\ \ldots,\ t \quad (3)$$

In equation (3), a represents the center of the membership function. d represents the width of membership function. The fuzzy rule calculation layer mainly adopts the fuzzy continuous multiplication in equation (4) to calculate the fuzzy degree. Each node in it is a fuzzy rule.

$$\varpi^j = \gamma_{(B_i^1)}(p_1) * \gamma_{(B_i^2)}(p_2) * \cdots * \gamma_{(B_i^m)}(p_m),\ i = 1,\ 2,\ \ldots,\ t \quad (4)$$

In equation (4), γ indicates membership degree. ϖ indicates the membership product of input parameters. The final output layer mainly outputs the actual predicted output value of the fuzzy neural network.

$$q_j = \frac{\sum_{j=1}^{o} \varpi^j(q_j)}{\sum_{j=1}^{o} \varpi^j} \quad (5)$$

The core of fuzzy clustering algorithm lies in calculating membership degree, which divides each data point into different clusters. Each data point is assigned a membership value, indicating the degree to which the point belongs to each cluster. In general, the membership value is a real number that ranges from [0,1]. In the fuzzy clustering algorithm, each data point is assigned to a different cluster and assigned a membership value that describes the similarity between the point and the cluster. If the membership value is high, the point is closer to the cluster center, which belongs more to the cluster. The Gaussian membership function is used for analysis, considering the interference degree F_i of i input and the preceding fuzzy set $\mu_{F_i}(x_i)$ in the fuzzy rule. The membership function shown in equation (5) is provided.

$$\mu_{F_i}(x_i) = exp\left[-\frac{\left(x_i - m_{F_i}\right)^2}{2{\sigma_{F_i}}^2}\right] \quad (6)$$

In equation (6), σ is the extension of the fuzzy set. If the value is large, the noise contained in the data will be even greater. Among them, the parameters that the T-S fuzzy neural network model actually needs to learn include the center and width of the membership function. They are calculated based on three steps, error calculation, neural network coefficient correction, and parameter correction. The error calculation is shown in equation (7).

$$w = \frac{1}{2}\left(h_e - h_f\right)^2 \quad (7)$$

In equation (7), w represents the error value between the expected output and the actual output. h_e and h_f represent the expected and actual output of the network. The network coefficient regularization corrects various parameters in the network based on the deviation between the expected output and the actual output, as expressed in equation (8).

$$\begin{cases} s_i^j(m) = s_i^j(m-1) - \Im\frac{\partial w}{\partial s_i^j} \\ \frac{\partial w}{\partial s_i^j} = \frac{(h_e - h_f)\varpi^j}{\sum_{j=1}^{m} \varpi^j p_i} \end{cases} \quad (8)$$

In equation (8), s_i^j represents the neural network coefficient. $\Im$ represents the network learning rate. Finally, the parameter correction is shown in equation (9).

$$\begin{cases} a_i^j = a_i^j(m-1) - \alpha\frac{\partial w}{\partial a_i^j} \\ d_i^j = d_i^j(m-1) - \alpha\frac{\partial w}{\partial d_i^j} \end{cases} \quad (9)$$

In equation (9), α represents a hyper-parameter. Based on the hydraulic motor fault pre-diagnosis, the main body and fault diagnosis in the entire lifecycle state assessment process are analyzed.

Among the classical CNNs, there are mainly LeNet-5, AlexNet, VGGNet and ResNet. Compared with other network structures, the residual structure of ResNet can directly connect the input data information and transmit it to the output, which solves the gradient disappearing and accuracy decreasing with the increase of layers. The architecture of ResNet-18 artificial neural network is shown in Figure 2. ResNet-18 has been trained on millions of images, which has rich feature representation capabilities. Figure 2 shows 4 residual blocks, each of which has two layers, each containing two 3*3 convolution layers. In addition to Conv1 and fully connected classification layers, there are a total of 18 layers. The explicit list of input and output parameters for ResNet-18 is shown in Table 1. In the figure, the residual structure has two layers. The input is learned by residual to form residual function. When the number of channels changes from 64 to 128, it is a dashed connection. At this time, the shortcut makes a linear change to x to adjust the dimension of the channel. From the residual network structure, the first 17 layers are feature extraction layers, and the 18th layer is classification layer. The fuzzy set defined for a single parameter includes N

types.

The theory domain of the classified object is $X = [x_1, x_2, \cdots, x_n]$. Each object has an index a to represent its properties, which is $X_i = (x_{i1}, x_{i2}, \cdots, x_{ij}), i = (1,2, \cdots, t)$.

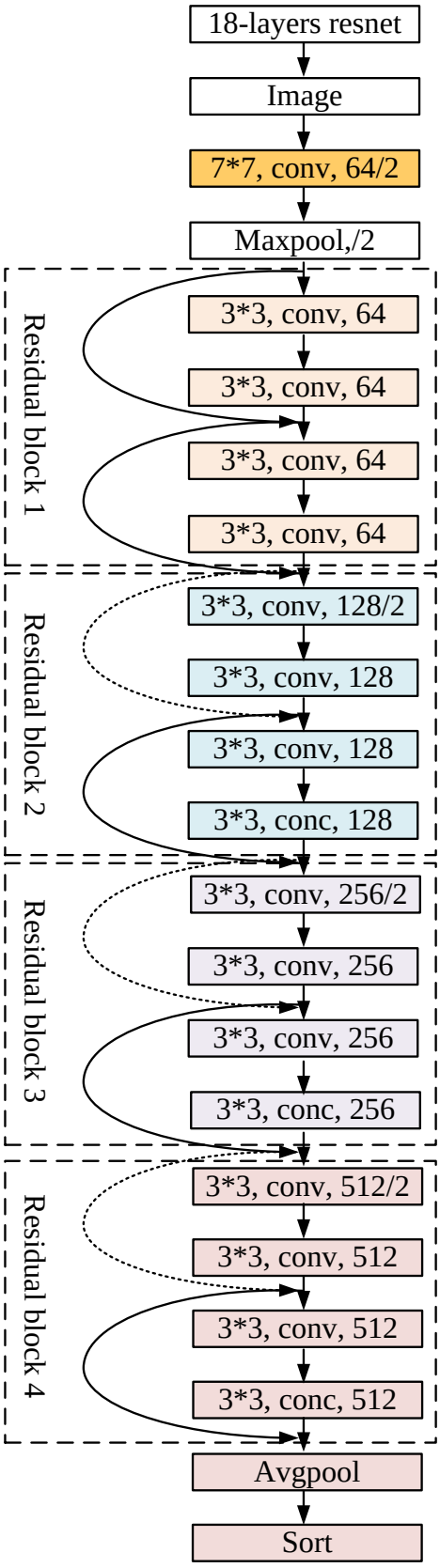

Figure 2. Resnet network structure.

The corresponding fuzzy set matrix is shown in equation (10).

$$X = \begin{bmatrix} x_{11} & x_{12} & \cdots & x_{1j} \\ x_{21} & x_{22} & \cdots & x_{2j} \\ \vdots & \vdots & & \vdots \\ x_{n1} & x_{n2} & \cdots & x_{nj} \end{bmatrix} \quad (10)$$

Table 1. Convolution layer input and output parameter details.

Input	**3*224*224**
/	64*112*112, k=7,s=2,p=3
	64*56*56, k=3,s=2,p=1
Residual block 1	64*56*56, k=3,s=1,p=1
	64*56*56, k=3,s=1,p=1
	64*56*56, k=3,s=1,p=1
	64*56*56, k=3,s=1,p=1
Residual block 2	128*28*28, k=3,s=2,p=1
	128*28*28, k=3,s=1,p=1
	128*28*28, k=3,s=1,p=1
	128*28*28, k=3,s=1,p=1
Residual block 3	256*14*14, k=3,s=2,p=1
	256*14*14, k=3,s=1,p=1
	256*14*14, k=3,s=1,p=1
	256*14*14, k=3,s=1,p=1
Residual block 4	512*7*7, k=3,s=2,p=1
	512*7*7, k=3,s=1,p=1
	512*7*7, k=3,s=1,p=1
	512*7*7, k=3,s=1,p=1
Output	512*1*1

The Resnet network is introduced to carry out the corresponding extraction to study the whole life cycle characteristics of hydraulic motors. The main reason is that the residual structure of Resnet can directly connect the input data information to the output, solving the gradient disappearance and accuracy declining with increasing layers. The actual parameters in the fully connected layer of the Resnet network account for the majority of the total parameters in the entire network, which also lead to low training speed and easy fitting problems [25]. Therefore, a GAP layer is introduced to replace the fully connected layer,

thereby improving the Resnet network to obtain Resnet-GAP. The architecture of GAP and fully connected layer is shown in Figure 3.

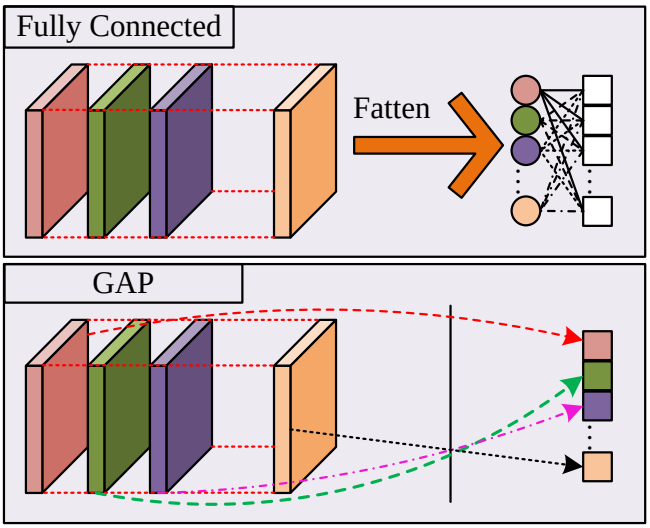

Figure 3. Architecture diagram of GAP and fully connected layer

From Figure 3, GAP can replace the fully connected layer to output features of any dimension as one-dimensional features. This enhances the feature extraction ability of the convolutional layer while retaining the spatial information extracted by the convolutional and pooling layers. At the same time, it can also adaptively adjust according to the feature dimensions and categories of hydraulic motor bearings, generating feature maps for each category in the classification after multi-layer perceptrons. Each feature map is globally averaged. An adaptive matrix is designed on the GAP structure. The size representation of the input feature map in the previous convolutional layer is shown in equation (11).

$$C_{out} = \frac{C_{in}-J}{stride} + 1 \tag{11}$$

In equation (11), C_{out} represents the size of the input feature map for the previous convolutional layer. C_{in} represents the size of the input feature map for the convolutional layer. J represents the size of the convolution kernel. $stride$ represents the step size. For the feature map input to GAP in the previous convolutional layer, the pooling core of GAP is automatically match with the number and dimension of convolutional cores. By pooling the feature map, a global mean equivalent to the fuzzy neural network is obtained, which is used as the feature value output by GAP. The operation expression of GAP is shown in equation (12).

$$Z_{avg-pool}^{l} = \frac{1}{\kappa}\sum_{k=1}^{\kappa} \Re_{1:g,1:f,k}^{l} \tag{12}$$

In equation (12), $Z_{avg-pool}^{l}$ represents the actual mean obtained by the l-th convolutional layer GAP. κ represents the number of neurons. $\Re_{1:g,1:f,k}^{l}$ represents the pixels in the actual mapping range of the output feature map corresponding to the mean pooling kernel, from the first row to the g row, and from the first column to the f column.

3.2. Post fault diagnosis for hydraulic motors

In this paper, Fuzzy Clustering Algorithm (FCA) is used to replace Softmax layer classification of Resnet-GAP network. The overall framework of hydraulic motor fault identification combining residual network and fuzzy clustering is shown in Figure 4. The power curve image of the switch machine is monitored and collected by microcomputer. The acquired image is input into the pre-trained Resnet-GAP model. The feature vector is output at the GAP layer to establish the typical power curve feature vector library of normal, sub-healthy, faulty and serious faults. FCA is used to replace the classification of the full connection layer and Softmax layer to realize fault identification.

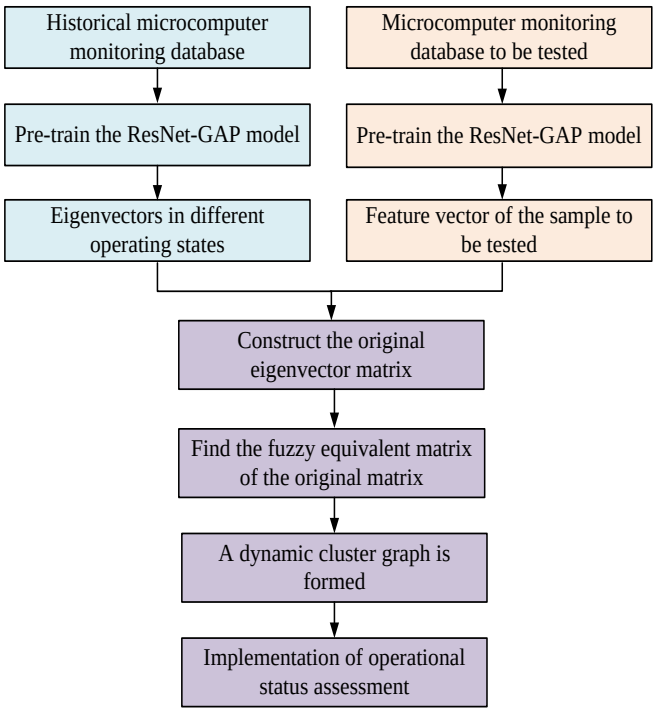

Figure 4. General framework for hydraulic motor fault identification.

On the basis of Resnet-GAP, the FCA in the fuzzy theory

used for fusion diagnosis prediction is studied to further optimize it for training with small sample data. Fuzzy clustering is an unsupervised learning method. The biggest advantage is that it does not require "learn" a large number of training samples. Similar objects can be gathered together through fuzzy operations alone [26]. This method introduces the concept of fuzzy mathematics in cluster analysis. On this basis, a similarity index is introduced. A fuzzy equivalence matrix is obtained by correcting the transfer closure method. A dynamic clustering graph is obtained when the elements in the transitive closure are from 0 to 1. The specific process is shown in Figure 5.

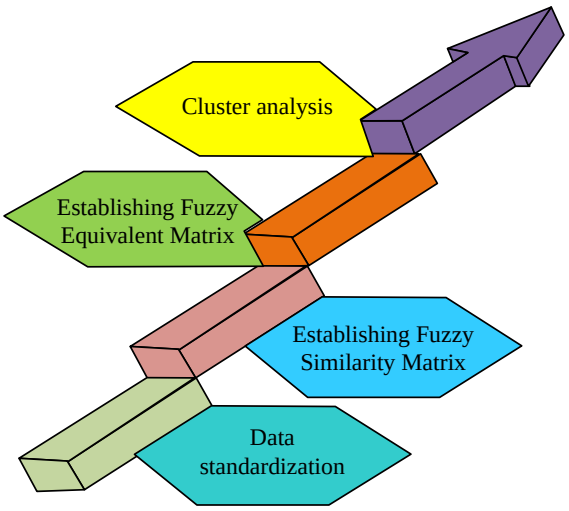

Figure 5. Schematic diagram of the clustering process of fuzzy clustering algorithm.

From Figure 5, the dynamic clustering process of the FCA first involves standardizing the data, followed by constructing a fuzzy similarity matrix, then constructing a fuzzy equivalence matrix, and finally conducting clustering analysis. Among them, the data matrix obtained after data standardization operation is displayed in equation (13).

$$N = \begin{bmatrix} n_{11} & n_{12} & \cdots & n_{1v} \\ n_{21} & n_{22} & \cdots & n_{2v} \\ \vdots & \vdots & \ddots & \vdots \\ n_{b1} & n_{b1} & \cdots & n_{bv} \end{bmatrix} \quad (13)$$

In equation (13), N represents the data matrix. n represents the internal elements of the matrix. b represents the elements within the domain of the classified object, with a maximum value of L. v represents the indicator, that is, the behavior. After transforming the translation standard deviation of equations (12) and (13), the actual influence of dimensionality between data can be eliminated, but there are still some $n'_{b\varsigma}$ that do not belong to (0,1). Therefore, a translation range transformation is also performed on them, as expressed in equation (14).

$$n''_{b\varsigma} = \frac{n'_{b\varsigma} - \min\limits_{1\le b\le L}\{n'_{b\varsigma}\}}{\max\limits_{1\le b\le L} n\{n'_{b\varsigma}\} - \min\limits_{1\le b\le L}\{n'_{b\varsigma}\}} \quad (14)$$

In equation (14), $n''_{b\varsigma}$ represents the data n after translation range transformation. After undergoing translation standard deviation and translation range transformation, all $n'_{b\varsigma}$ belong to (0,1), thus eliminating the influence of dimensionality. In response to the different dimensions caused by different data and the data requirements for adapting to fuzzy clustering, data n is subjected to translation standard deviation and translation range transformations. The translation standard deviation transformation is expressed as equation (15).

$$n'_{b\varsigma} = \frac{n_{b\varsigma} - \bar{n}_{\varsigma}}{s_{\varsigma}} \quad (15)$$

In equation (15), $n'_{b\varsigma}$ represents the result of data n translation transformation. s_{ς} represents the translation standard deviation transformation result. $\bar{n}_{\varsigma}$ represents the average value of indicator ς in data n.s_{ς} and $\bar{n}_{\varsigma}$ are shown in equation (16).

$$\bar{n}_{\varsigma} = \frac{1}{L}\sum_{b=1}^{L} n_{b\varsigma}, s_{\varsigma} = \sqrt{\frac{1}{L}\sum_{b=1}^{L}\left(n_{b\varsigma} - \bar{n}_{b\varsigma}\right)^2} \quad (16)$$

In addition, after data standardization, the corresponding fuzzy matrix can be obtained. However, to achieve further clustering, the similarity between samples is calculated. Therefore, the study constructs a fuzzy similarity matrix. The distance method determines the similarity between samples, as expressed in equation (17).

$$R_{bz} = 1 - \psi C(n_b, n_z) \quad (17)$$

In equation (17), R_{bz} represents the similarity between samples. ψ represents a definite constant. $C(n_b, n_z)$ represents the distance between two samples. z represents the elements in the domain of the classified object that is not equal to b. The $C(n_b, n_z)$ can be determined by Hamming distance and Euclidean distance, as shown in equations (18) and (19).

$$C(n_b, n_z) = \sum_{\varsigma=1}^{\Psi}\left|n_{b\varsigma} - n_{z\varsigma}\right| \quad (18)$$

In equation (18), Ψ represents the number of indicators.

$$C(n_b, n_z) = \sqrt{\sum_{\varsigma=1}^{\Psi}\left(n_{b\varsigma} - n_{z\varsigma}\right)^2} \quad (19)$$

After comprehensive consideration, the Euclidean distance method is chosen to determine the similarity between samples.

Finally, in cluster analysis, the similarity expression between the element samples in the transitive closure is shown in equation (20).

$$R_{bz}(\delta) = \begin{cases} 1, R_{bz} \geq \delta \\ 0, R_{bz} \leq \delta \end{cases} \quad (20)$$

In equation (20), δ represents the element in the transitive closure. Finally, the entire life cycle state assessment process of the constructed hydraulic motor is shown in Figure 6.

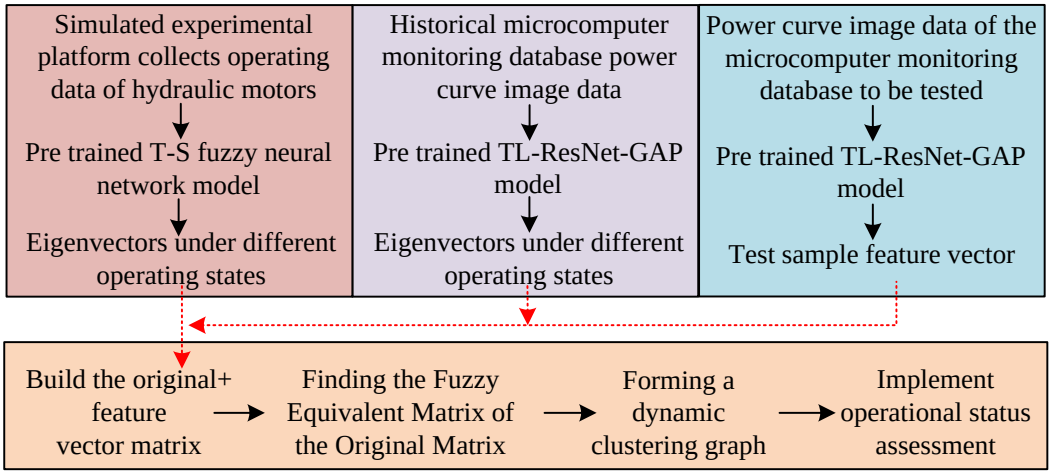

Figure 6. Process for evaluating the full life cycle status of hydraulic motors.

From Figure 6, real-time monitoring of the hydraulic motor operation process is achieved through the microcomputer monitoring technology in this process. The power curve and flow data curve of the hydraulic motor during operation are obtained. Then it is input into the pre-trained Resnet-GAP model and T-S fuzzy neural network model, and output feature vectors in the GAP layer. Feature vectors under typical working conditions such as normal, sub healthy, faulty, and severe faults are constructed. The fuzzy clustering method is used to replace the complete connection layer and software maximum level classification, evaluating the hydraulic motor status. On this basis, the identification under sub healthy conditions is introduced. The parameters of the GAP layer are trained using small samples to improve the feature extraction ability, achieving effective operating status identification for hydraulic motors. In addition, to enhance the universality of the model, a dense connection network (Densenet) with a deeper network structure and stronger feature extraction ability is used for experimental verification. Pre-trained Fine-Tuning (TL) and GAP are used to replace fully connected layers. At the same time, FCM is used to replace the maximum softening classification layer in the network. An activation function is used when GAP proposes feature outputs to construct the TL-Densenet-GAP-FCM model.

To monitor the pressure and flow of the hydraulic motor, the study adopts computer-aided testing technology to install pressure sensors and flow sensors in the hydraulic circuit. By monitoring the pressure and flow of the hydraulic circuit and the hydraulic motor, the differences between these parameters in the normal working state and the leakage fault state are compared. The changes in parameters are recorded. It provides data support for the training of hydraulic motor internal leakage fault prediction model. The prediction model based on fuzzy neural network is established in MATLAB. The output current of the magnetic powder brake controller is fixed at 0.1A and the load remains constant. The experimental data obtained by changing the throttle opening is used for fault prediction.

4. Performance verification of T-S fuzzy neural network model and Resnet-GAP-FCM model

To verify the actual effectiveness of the proposed T-S fuzzy neural network model in pre-fault prediction and the Resnet-GAP-FCM model in post fault diagnosis, experiments are conducted in this section.

4.1. Performance verification of T-S fuzzy neural network model

The operating system used in this experiment is Ubuntu22.04. The development language is Python • 3.8.0; The framework

is Pytorch 1.10.0-+ cuda.11.1, and the CPU is Intel • Xeon Gold-6138. The GPU is GeForce • RTX • 3090(24G). Memory 220G. The CY14-1B piston pump with rated pressure of 31.5Mpais selected as the power element of the simulation test bench. According to the torque that the motor can provide under the extreme working conditions, the model FZ100A-1 magnetic powder brake is selected. To ensure that the flow adjustment range is large enough and the action is sensitive when adjusting the throttle opening, the throttle valve model LA-H10L is adopted. To ensure that the hydraulic pressure does not exceed the maximum allowable value of 31.5MPa, the simulation test bench uses the direct acting relief valve model YP-L10H4, the pressure relay model HJCS-02N produced by Taiwan HDX Company, and the electromagnetic directional valve model D5-2B60B-D2 produced by RISUNY Company. Finally, the NI USB-6008 data acquisition card developed by the National Instruments Company of the United States is selected for data acquisition, and the acquisition accuracy is 12 bits.

The open dataset of bearings from Case Western Reserve University in the United States is used to validate bearing fault diagnosis under the same model and operating conditions. 7 types of bearing fault data including 12kHZ drive end, motor speed of 1797r/min, fault diameter of 0.007 and 0.021, inner ring fault, roller fault and normal state are taken as examples. There are 20 samples in each group, a total of 140 groups, for experimental verification. The fuzzy logic controller takes 1000 continuous points from the time domain signal as samples to establish a standard data vector library, as shown in Table 2, D1, D2, D3, and D4 are the numbers of the data to be measured.

Table 2. Standard database sample characteristics.

Sample to be tested	1	2	3	…	1919	1920
D1	-2.46	-2.50	8.23	…	0.43	-0.76
D2	-2.56	-4.62	1.10	…	0.75	-0.34
D3	-2.60	-9.92	-6.43	…	-0.78	-0.26
D4	-1.82	0.01	1.44	…	-0.23	0.64

Based on predictions and true labels, the samples are divided into four categories: True Positive (TP), True Negative (TN), False Positive (FP) and False Negative (FN). The accuracy of hydraulic motor fault identification, recall rate and F1 value are calculated to verify the performance. The specific results are shown in Figure 7.

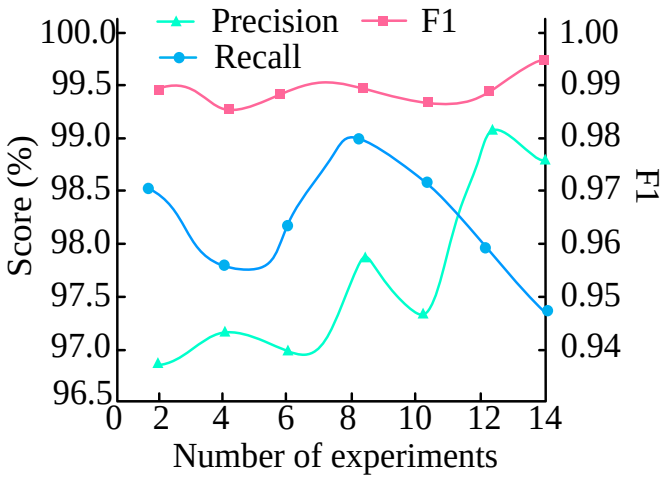

Figure 7. Hydraulic motor fault detection and classification

accuracy analysis.

The hydraulic motor fault identification model has good performance, which can accurately detect faults. The accuracy of each test was more than 96%, most of them reached 97% and 98%, and the highest even was 99.2%. The recall rate was more than 97%, and the highest was 99.2%. F1 value was relatively stable in many experiments, with each experiment above 0.98. The average value of 10 experiments was 0.989. The specific operation of the experiment is as follows. 14 data (numbered 1-1~1-14)are randomly selected from 144 actual data collected in this group to verify the prediction accuracy. The first 50, 60, 70, 80, 90, 100, 110, 120 and 130 data are used for the model training to compare the prediction accuracy under different combinations.

To reduce the complexity of the study, different numbers of data samples are represented as 50-14, 60-14, ..., 130-14 (represented by 1-9) for training and validating the prediction model. Among them, the model prediction results and relative error results are shown in Figure 8.

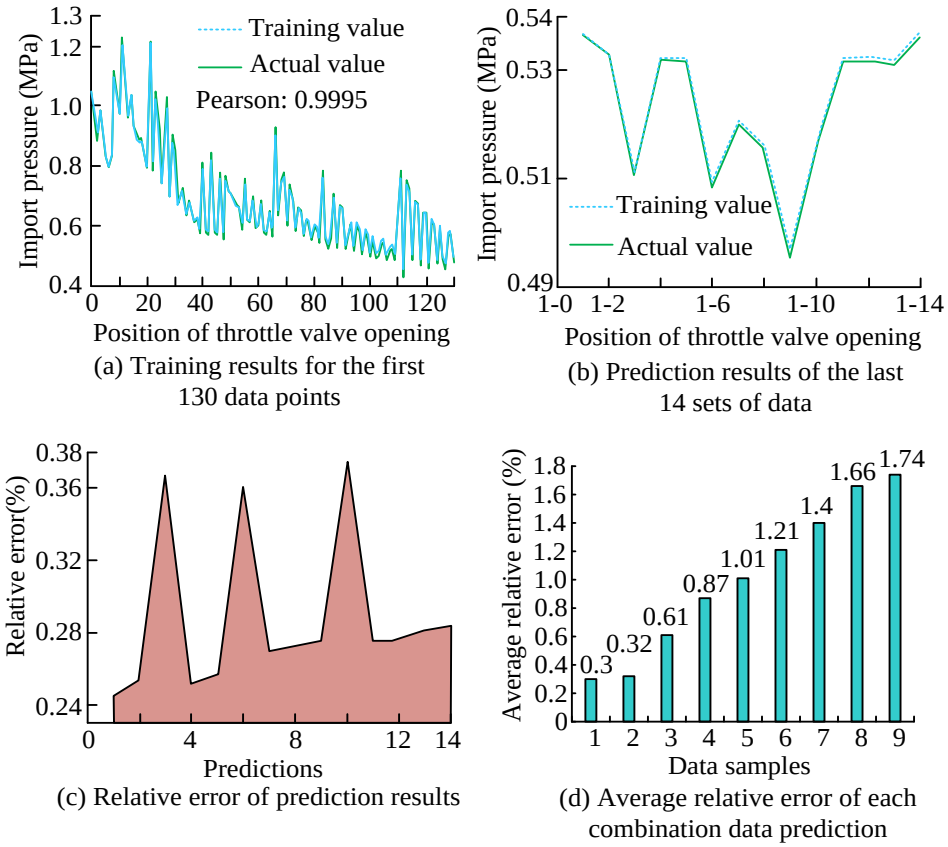

Figure 8. Model prediction results and relative error results.(a) Training results for the first 130 data points. (b) Prediction results of the last 14 sets of data. (c) Relative error of prediction results. (d) Average relative error of each combination data prediction.

From Figure 8 (a), the curve between the training values and the actual values was basically consistent. The Pearson correlation coefficient between two values was 0.9995, indicating a highly correlation between the two. The actual training effect of the model was good. From Figure 8 (b), the last 14 sets of predicted results showed that the predicted values were generally consistent with the actual value curve. From Figure 8 (c) and (d), the actual prediction error gradually increased with the increase of prediction compensation. The relative error was also relatively large in positions where there were significant fluctuations in the data. The maximum relative error of the actual prediction was 0.38%. The average relative error of all 14 prediction results was 0.30%. Overall, after training with a large number of data samples, the prediction accuracy of the model is high. However, the accuracy improvement rate decreases significantly after exceeding 120 samples. Therefore, 120 samples for model training has the best effect, but it also proves the effectiveness of the T-S fuzzy neural network model in hydraulic motor fault prediction.

Large fluctuations in data may affect the training and prediction performance of the model, resulting in a significant deviation between the predicted results and the true values. Therefore, this study uses data fitting to smooth the experimental data, reducing areas with relatively large fluctuations in the data. In the experiment, the Smoothing Splines in the matrix laboratory fitting toolbox is used to fit the relevant parameters. The relevant parameters and the fitting curve results are shown in Figure 9

From Figure 9 (a), there were 4 fitting parameters, namely residual sum of squares, determination coefficient, correction determination coefficient, and root mean square error, with values of 0.516, 0.877, 0.735, and 0.088, respectively. From Figure 9 (b), the fitting curve maintained the inlet pressure of the hydraulic motor between 0.5 and 1.15Mpa at the throttle threshold opening of 0 to 140, showing a fluctuating downward trend. Then the training and prediction results of the fitted model are shown in Figure 10.

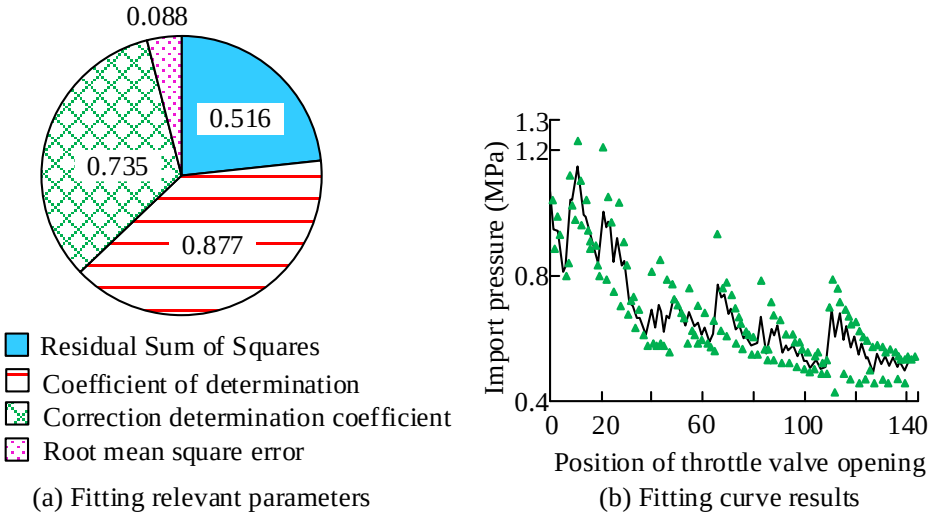

(a) Fitting relevant parameters (b) Fitting curve results

Figure 9. Related parameter content and fitting curve results.(a) Fitting relevant parameters. (b) Fitting curve results.

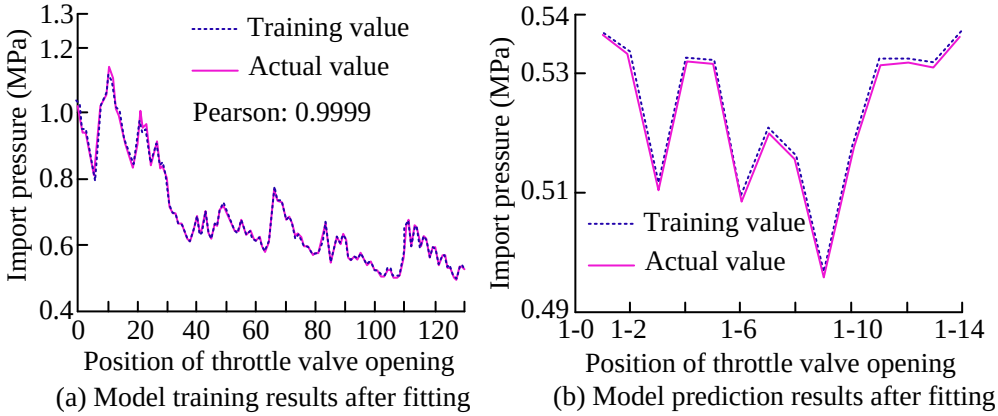

(a) Model training results after fitting (b) Model prediction results after fitting

Figure 10. Model training and prediction results after fitting.(a) Model training results after fitting. (b) Model prediction results after fitting.

From Figure 10 (a), the Pearson correlation coefficient of the fitted model was 0.9999. The correlation between the fitting training values and the actual values was compared. It indicated that the actual training effect of the model was better. From Figure 10 (b), the difference between the predicted and actual values in the fitted prediction results did not exceed 0.4%. The difference between inlet pressures was very small. The predicted relative error and average relative error are shown in Figure 11.

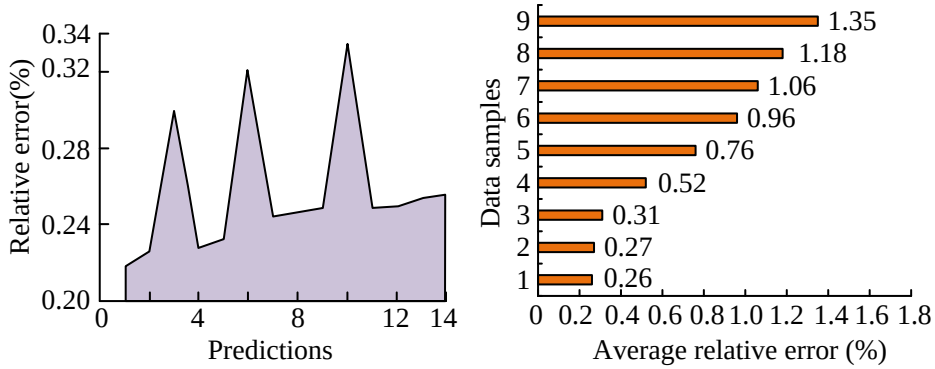

(a) Relative error of predicted results after fitting (b) Predicted average relative error after fitting

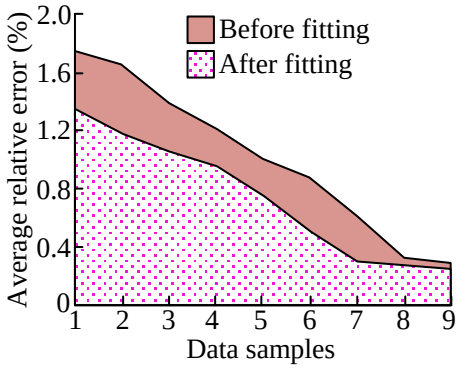

(c) Comparison of average relative error before and after fitting

Figure 11. Relative error and average relative error predicted after fitting.(a) Relative error of predicted results after fitting. (b) Predicted average relative error after fitting. (c)Comparison of average relative error before and after fitting.

From Figures 11 (a) and (b), the maximum relative error between the predicted value and the actual value was 0.334%. The average relative error was 0.257%. There was a significant decrease compared with before fitting, indicating an improvement in the prediction accuracy. From Figure 10 (c), compared with before fitting, the fitted model had a lower average relative error and higher prediction accuracy under the same training data samples. For the fitted data, the prediction accuracy of the model was improved by at least 15% compared to before fitting. Overall, the prediction model proposed in the study had effectiveness and high accuracy in predicting hydraulic motor faults. To further verify the results, CNN, the algorithm that integrates short-time Fourier and support vector machine, the algorithm that integrates extreme gradient boosting and long short-term neural network, and fast recurrent neural network algorithm are introduced for comparison. The comparison algorithms are represented by A-D. The comparison results of fault prediction accuracy are shown in Table 3.

Table 3. Comparison of fault prediction accuracy of hydraulic motors using different algorithms.

-	Accuracy (%)	Precision (%)	Recall (%)	F1 value (%)
A	64.99	65.16	64.99	65.09
B	82.06	82.27	82.06	82.17
C	85.77	85.87	85.76	85.82
D	81.25	81.35	81.24	81.30
Research model	96.15	96.17	96.15	96.16

From Table 3, the accuracy of the research model in predicting hydraulic motor faults reached 96.15%. The precision was 96.17%, the recall rate was 86.15%, and the F1 value was 96.16%, all of which were higher than the comparison models. Overall, the T-S fuzzy neural network model proposed in the study has high performance in hydraulic motor fault prediction.

4.2. Performance verification of Resnet-GAP-FCM model

To verify the diagnostic accuracy of Resnet-GAP-FCM model, the bearing open data set of Case Western Reserve University in the United Statesis used in this study. The bearing fault diagnosis under the same model and working condition is verified by the algorithm presented in this paper. 7 types of bearing fault data including 12kHZ drive end, motor speed of 1797r/min, fault diameter of 0.007 and 0.021 are taken as examples for experimental verification. Taking 1000 continuous points from time domain signal as samples, a standard database is established for fault simulation experiment. To ensure that the key parameters in the experimental environment are consistent with the real environment, the key parameters in the hydraulic motor modeling in the laboratory are consistent with the actual changes. The phenomenon and process in the experimental environment are verified by mathematical model and computer simulation. The experiment mainly evaluates whether the actual operation of the motor meets the requirements of rated power, theoretical speed, oil leakage capacity, vibration noise, etc. Meanwhile, it can simulate

faults such as wear of hydraulic motor rollers and stator rings, as well as cracks in rollers and stator rings. Firstly, the time-domain analysis method is used to draw the vibration signals of hydraulic motors in different states, providing a basis for subsequent model diagnosis. When a composite fault occurs, the vibration signal results of the hydraulic motor are shown in Figure 12.

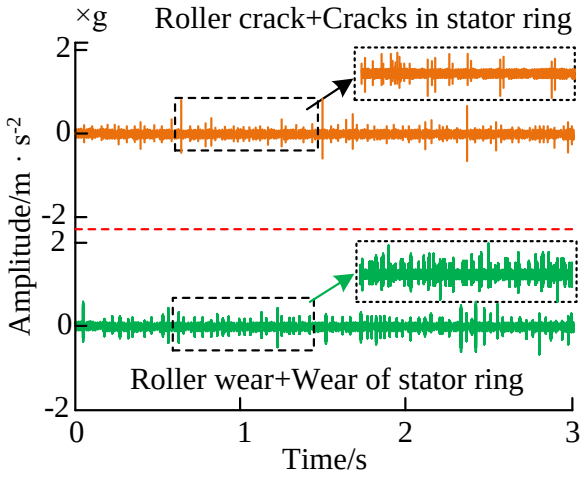

(a) Signal of roller wear plus wear of stator ring and roller crack plus cracks in stator ringstator crack

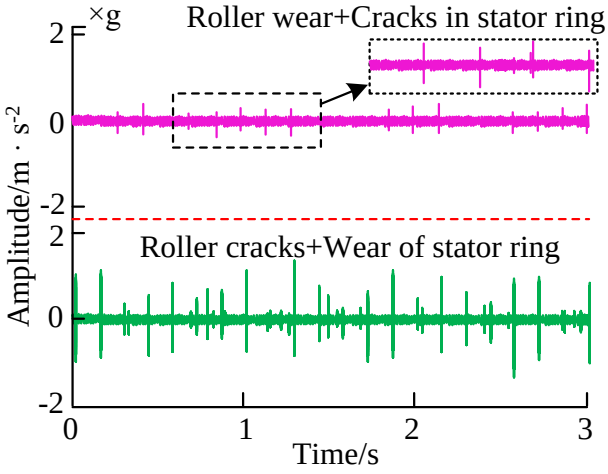

(b) Signal of roller crack plus wear of stator ring and roller wear plus cracks in stator ring

Figure 12. Vibration signals of hydraulic motors during composite faults. (a) Signal of roller wear plus wear of stator ring androller crack plus cracks in stator ring stator crack. (b) Signal of roller crack plus wear of stator ring and roller wear plus cracks in stator ring.

From Figures 12 (a) and (b), when both the hydraulic motor roller and stator ring failed simultaneously, the impact characteristics were more pronounced compared to normal signals. Among them, the amplitude when both the roller and stator ring wear faults occurred simultaneously was ±0.6g, significantly higher than the normal signal. When both the roller and stator ring cracked simultaneously, the amplitude was ±0.6g. However, the actual vibration impact was more severe. The amplitude when roller wear and stator ring cracks occurred simultaneously was ±0.4g. When roller cracks and stator ring wear occurred simultaneously, the amplitude was ±1.5g, and the impact characteristics were most significant. The vibration signals of hydraulic motors contain rich health status information. The time-domain indicators can quantitatively evaluate the health status of hydraulic motors. Therefore, after analyzing the kurtosis, peak, and pulse factors, the health status of hydraulic motors can be further evaluated. The specific content is shown in Table 4.

Table 4. The kurtosis, peak value, and pulse factor results of normal and fault signals for hydraulic motors.

-	E	F	G	H	I	-	F+G	H+I	H+G	F+I
Q	2.87	14.45	4.71	168.04	84.51	Q	8.59	49.89	100.79	23.54
Z	9.29	20.04	12.30	47.28	38.23	Z	21.11	36.53	40.17	25.83
M	11.49	29.94	16.01	86.85	69.27	M	28.86	60.35	89.37	38.81

In Table 4, E-I represent normal state, roller wear, stator ring wear, roller cracks, and stator ring cracks. Q, Z and M represent kurtosis, peak, and pulse factors. From Table 4, when the hydraulic motor rollers worn or cracked, their kurtosis coefficient, peak coefficient, and impulse coefficient all underwent significant changes. The kurtosis coefficient is 5 times higher than the normal value. The peak coefficient was 58 times higher than normal, indicating significant impact characteristics. In a single fault, the index of rolling crack fault in the time domain was the largest. The composite fault time domain index indicated that there was a significant variation in the time domain index of hydraulic motors with both roller cracks and stator ring wear, but its amplitude was much smaller. The proposed Resnet-GAP-FCM model is applied to the fault diagnosis of hydraulic motors. In this experiment, the data of each type of fault was integrated into

a group to expand the total fault samples, with the training set accounting for 50%, the validation set accounting for 25%, and the test set accounting for 25%. The content of the hydraulic motor experimental dataset and the confusion matrix for fault diagnosis are shown in Figure 13.

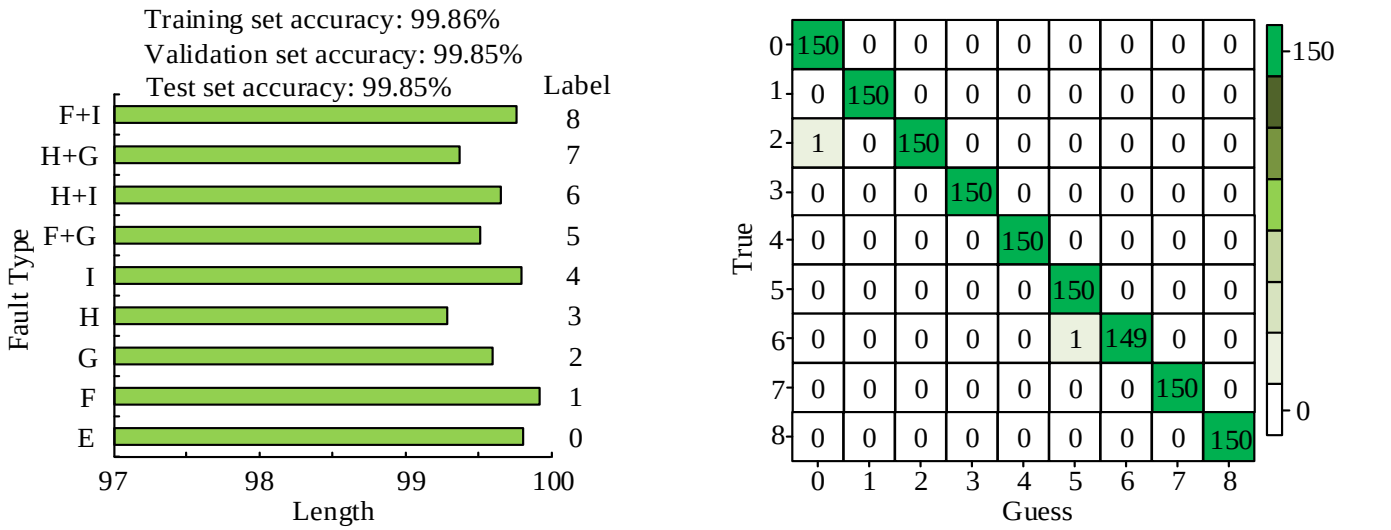

(a) The length and label of different types of faults (b) Confusion Matrix for Hydraulic Motor Fault Diagnosi

Figure 13. Content of hydraulic motor experimental dataset and confusion matrix for fault diagnosis.(a) The length and label of different types of faults. (b) Confusion Matrix for Hydraulic Motor Fault Diagnosis.

From Figure 13 (a), the accuracy of the training, validation, and testing sets of the model after training was higher than 99.8%, indicating that the proposed model had strong feature extraction and fault diagnosis capabilities. From Figure 13 (b), he research model had a high accuracy in diagnosing faults in hydraulic motors. Overall, the research model has high performance in hydraulic motor fault diagnosis. On this basis, the fault diagnosis results of hydraulic motors are visualized to assess the clustering and classification ability of the research model, as shown in Figure 14.

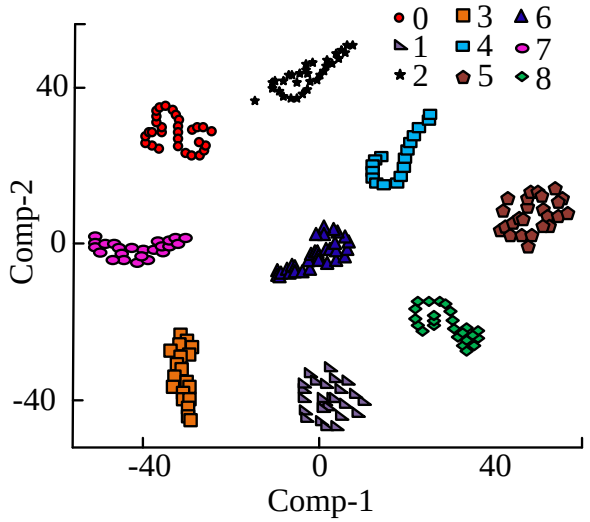

Figure 14. Visualization results of hydraulic motor fault diagnosis.

In visual fault location, fault location can be divided into two stages. Before the failure stop loss, it is expected that the information can be quickly obtained for stop loss decision. The corresponding stop loss operation can be made to restore the service. After the fault stop loss, it is still necessary to further find the deep-seated cause of the fault, determine the root cause of the fault, and restore the online environment to normal state. From Figure 14, the improved model retained the feature extraction capability of the convolutional layer. A deeper level network can be selected based on the complexity of the detection target curve. Training samples are added appropriately to improve classification accuracy, so that the model can quickly detect changes that may cause faults. To further verify the diagnostic superiority of the proposed hydraulic motor, the Fusion Algorithm of Radial Basis Function and Support Vector Machine (FARF-SVM) [27], CNN and Support Vector Machine (CNN-SVM) [28], Classification and Regression Tree (CRT) algorithm [29], Artificial Neural Network algorithm (ANN) [30] and CNN [31] are introduced to compare the diagnostic classification accuracy. The results are shown in Table 5.

Table 5. Comparison of accuracy of different algorithms in diagnosing and classifying hydraulic motors.

-	Total number of training samples	Iterations	Accuracy (%)
FARF-SVM	300.00	-	97.25
CNN-SVM	500.00	140.00	97.51
CRT	300.00	-	93.55
ANN	490.00	1000.00	96.52
CNN	3050.00	-	97.45
-	Total number of training samples	Iterations	Accuracy (%)
Resnet-GAP-FCM	160.00	100.00	99.00
TL-Densenet-GAP-FCM	160.00	100.00	99.05

From Table 5, the diagnostic classification accuracy of the Resnet-GAP-FCM model proposed in the study was 99.00%, which was higher than the comparison algorithms. Meanwhile, to enhance the model universality, the improved TL-Densenet-GAP-FCM model had a diagnostic classification accuracy of 99.05, proving the certain universality. Overall, out of a total of 3050 samples, only 160 samples obtained by the research model were higher than the CNN algorithm, indicating the superiority of the research model in small samples.

Table 6 summarizes the main test results of the proposed model. The prediction results of the model are compared with the remaining experimental data. The results indicated that if there were more data samples used for model training, the prediction accuracy is higher. Large data fluctuations could affect the prediction accuracy of the model. The original experimental data was fitted. Compared with the experimental data before fitting, and the same experimental data was used to verify the prediction accuracy before and after fitting to ensure the credibility of the verification results. After fitting the experimental data with the fitting method selected in this paper, if there were more training samples, the prediction accuracy of the model is higher. The prediction accuracy of the model was at least 15% higher than that before fitting.

Table 6. Summary of main test results of the proposed model.

The main test index of the model	Result
Maximum relative error of model prediction results	0.38%
Average relative error value	0.30%
The difference between the predicted value and the actual value after fitting	<0.4%
The average relative error between the predicted and actual values	0.257%
Improvement of model prediction accuracy	>15%
Accuracy	96.15%
Precision	96.17%
Recall	86.15%
F1	96.16%
Diagnostic classification accuracy of ResNet-GAP-FCM model	99.00%

5. Discuss

In recent years, deep learning neural networks have been widely used in different fields, especially in image recognition, fault diagnosis, life prediction, etc., due to their strong ability of self-learning and feature information extraction [32]. Although the deep convolutional neural network can improve the classification accuracy to a certain extent, it will cause the gradient to disappear with the increase of the number of layers and cannot be trained. At the same time, a large amount of data is needed to train the model parameters during fault diagnosis. However, the fault data of hydraulic motors are few and difficult to obtain, which cannot meet the training requirements. Therefore, there are certain deficiencies in the fault diagnosis of hydraulic motors in practice [33]. Compared with the traditional method based on deep convolutional neural network, the most significant difference between the hydraulic motor fault diagnosis model built in this paper based on fuzzy clustering and improved Resnet network is that GAP layer is used to replace the fully connected network in Resnet, and fuzzy clustering replaces the classification layer of Resnet. Using a small amount of data to train the parameters of GAP layer, the feature extraction ability of the model is improved. It solves the problem of less training data and has the advantages of self-adaptation and small sample.

Based on the results of Table 4, 5 and 6, the hydraulic motor fault diagnosis proposed by the research based on the improved Resnet network has high detection accuracy, good

effect on fault signal processing, and high signal and noise after noise reduction. The fault features and the proposed automatic feature extraction method are used to extract the acoustic signal of synchronous hydraulic motor. Finally, the signal features are trained and classified by fuzzy clustering algorithm. The accuracy of the proposed fault diagnosis method based on the diagnosis results can reach more than 99%, and the final fault diagnosis accuracy will be affected to some extent when the pre-processing noise reduction effect is not ideal. The improved convolutional neural network has better feature extraction ability, uses a small number of samples to train the parameters of GAP layer, establishes the pre-trained model and fuses the fuzzy clustering algorithm. The proposed fault diagnosis method has certain robustness.

Existing diagnosis methods based on expert systems have low fault coverage and are difficult to identify new faults [34]. Compared with expert system, model-based fault diagnosis has a wider application range and better diagnostic effect. However, this method relies too much on the digitization of diagnostic objects, which makes it difficult to establish an accurate digital model in practical application [35]. The fault diagnosis method based on data and machine learning is the most widely used diagnosis technology at present. The fault characteristics can be extracted by data analysis and processing or the neural network can be trained by historical fault data to effectively identify equipment faults. Compared with the above methods, the Pearson correlation coefficient after fitting the model proposed in this study is 0.9999, indicating that the model has a good actual training effect. The difference between the predicted value and the actual value in the predicted results after fitting is less than 0.4%, and the accuracy of the training set, verification set and test set after model training are all higher than 99.8%, indicating that the research model has strong feature extraction and fault diagnosis capabilities. The accuracy of diagnosis classification is as high as 99.00%, and the results obtained by the research model with only 160 samples are higher than the results obtained by the algorithm N with a total of 3050 samples, which shows the superiority of the research model in small samples. In summary, the research model has high performance in hydraulic motor fault diagnosis.

6. Conclusion

The troubleshooting of hydraulic motors often focuses solely on fault prediction or diagnosis. Therefore, a comprehensive life cycle state evaluation method for hydraulic motors is proposed by integrating fuzzy logic theory and improved Resnet network. The effectiveness is verified. According to the experimental results, the Pearson correlation coefficient between the training value and the actual value was 0.9995, which was 0.9999 after fitting, indicating that the model training effect was good. The maximum relative error between the fitted predicted value and the actual value was 0.334%, with an average relative error of 0.257%. The fault prediction accuracy was 96.15%, which was better than the comparison models. In the verification of fault diagnosis model, the accuracy of the training set, verification set and testing set after model training was all higher than 99.8%, indicating that the research method had higher practicability. The number of training samples can be appropriately increased or decreased according to the complexity of the detection targetcurve, so as to improve the feature extraction capability of the convolutional layer, increase the classification accuracy and realize the detection of the target. In summary, the proposed method combining hydraulic motor fault prediction and diagnosis has high accuracy, which can complete classification without data training, with self-adaptation and small sample size. At the same time, the feature extraction capability of the convolutional layer can be retained. A deeper network can be selected according to the curve complexity of the detection target and appropriate training samples can be added to increase the classification accuracy. Extreme temperature will make the parts of the hydraulic motor expand or contract, resulting in increased friction and reduced efficiency. In this study, only the fault causes of the hydraulic motor were preliminarily located and analyzed, without considering the influence of the extreme temperature working environment. In the future, we can combine the power characteristics of the hydraulic motor during operation and the influence of the external environment to re-classify the health grade. At the same time, considering the performance degradation of the switch machine, the state degradation characteristics are extracted, the real-time hydraulic motor state evaluation system is established, the standard sample

database is improved, the probability of misjudgment and missing judgment is reduced, and the real-time monitoring of the operating state of the hydraulic motor is realized.

REFERENCE

1. Huang K, Wu S, Li F, Yang C, Gui W. "Fault diagnosis of hydraulic systems based on deep learning model with multirate data samples," IEEE Trans. Neural Netw. Learn. Syst., 2022; 33(11): 6789-6801, https://doi.org/10.1109/TNNLS.2021.3083401.
2. Qian Q, Luo J, Qin Y. "Adaptive intermediate class-wise distribution alignment: A universal domain adaptation and generalization method for machine fault diagnosis," IEEE Trans. Neural Netw. Learn. Syst., 2024; 1-15, https://doi.org/10.1109/TNNLS.2024.3376449.
3. Zhou J, Qi J, Chen D, Qin Y. "Continuous remaining useful life prediction by self-guided attention convolutional neural network and memory consciousness adjustment," IEEE Internet Things J., 2024; 11(19): 31947-31958, https://doi.org/10.1109/JIOT.2024.3421673.
4. Stojanovic V. "Fault-tolerant control of a hydraulic servo actuator via adaptive dynamic programming," Math. Model. Control, 2023; 3(3): 181-191, https://doi.org/10.3934/mmc.2023016.
5. Tang S, Zhu Y, Yuan S. "Intelligent fault diagnosis of hydraulic piston pump based on deep learning and Bayesian optimization," ISA Trans., 2022; 129(3): 555-563, https://doi.org/10.1016/j.isatra.2022.01.013.
6. Manikandan S, Duraivelu K. "Fault diagnosis of various rotating equipment using machine learning approaches-A review," Proc. Inst. Mech. Eng. Part E-J. Process Mech. Eng., 2021; 235(2): 629-642, https://doi.org/10.1177/0954408920971976.
7. Manikandan S, Duraivelu K. "Vibration-based fault diagnosis of broken impeller and mechanical seal failure in industrial mono-block centrifugal pumps using deep convolutional neural network," J. Vib. Eng. Technol., 2023; 11(1): 141-152, https://doi.org/10.1007/s42417-022-00566-0.
8. Askari B, Carli R, Cavone G, Dotoli M. "Data-driven fault diagnosis in a complex hydraulic system based on early classification," IFAC Papersonline, 2022; 55(40): 187-192, https://doi.org/10.1016/j.ifacol.2023.01.070.
9. Shi JC, Ren Y, Tang HS, Xiang JW. "Hydraulic directional valve fault diagnosis using a weighted adaptive fusion of multi-dimensional features of a multi-sensor," J. Zhejiang Univ.-Sci. A, 2022; 23(4): 257-271, https://doi.org/10.1631/jzus.A2100394.
10. Long Z, Zhang X, He M, Huang S, Qin G, Song D, Tang Y, Wu G, Liang W, Shao H. "Motor fault diagnosis based on scale invariant image features," IEEE Trans. Ind. Inform., 2022; 18(3): 1605-1617, https://doi.org/10.1109/TII.2021.3084615.
11. Lu S, Qian G, He Q, Liu F, Liu Y, Wang Q. "In situ motor fault diagnosis using enhanced convolutional neural network in an embedded system," IEEE Sens. J., 2020; 20(15): 8287-8296, https://doi.org/10.1109/JSEN.2019.2911299.
12. Ke Z, Di C, Bao X. "Adaptive suppression of mode mixing in CEEMD based on genetic algorithm for motor bearing fault diagnosis," IEEE Trans. Magn., 2022; 58(2): 8200706.1-8200706.6, https://doi.org/10.1109/TMAG.2021.3082138.
13. Long Z, Zhang X, Song D, Tang Y, Huang S, Liang W. "Motor fault diagnosis using image visual information and bag of words model," IEEE Sens. J., 2021; 21(19): 21798-21807, https://doi.org/10.1109/JSEN.2021.3102019.
14. Dai J, Tang J, Huang S, Wang Y. "Signal-based intelligent hydraulic fault diagnosis methods: Review and prospects," Chin. J. Mech. Eng., 2019; 32(1): 75.1-75.22, https://doi.org/ 10.1186/s10033-019-0388-9.
15. Sun W, Shao S, Zhao R, Yan R, Zhang X, Chen X. "A sparse auto-encoder-based deep neural network approach for induction motor faults classification," Measurement, 2016; 89(2): 171-178, https://doi.org/10.1016/j.measurement.2016.04.007.
16. Soni R, Mehta B. "Diagnosis and prognosis of incipient faults and insulation status for asset management of power transformer using fuzzy logic controller & fuzzy clustering means," Electr. Power Syst. Res., 2023; 220(14): 109256.1-109256.18, https://doi.org/10.1016/j.epsr.2023.109256.
17. Soni R, Mehta B. "Condition based assessment and diagnostics of transformer in smart grid network using adaptive neuro fuzzy inference system framework," Int. Manuf. Energy Sustainability, 2023; 372:139-150, https://doi.org/10.1007/978-981-99-6774-2_13.
18. Lima ALDD, Aranha VM, Nascimento EGS."Predictive maintenance applied to mission critical supercomputing environments: remaining useful life estimation of a hydraulic cooling system using deep learning," J. Supercomput., 2023; 79(4): 4660-4684, https://doi.org/10.1007/s11227-022-04833-5.
19. Shi Q, Hu Y. "Review on intelligent diagnosis technology of electronically controlled fuel injection system of ME diesel engine," Acad. J. Sci. Technol., 2022; 1(2): 69-75, https://doi.org/10.54097/ajst.v1i2.351.

20. Zhang Z, Li Z, Zhao C. "Research on condition monitoring and fault diagnosis of intelligent copper ball production lines based on big data," IET Collab. Intell. Manufact., 2022; 4(1): 45-57, https://doi.org/10.1049/cim2.12043.
21. Araste Z, Sadighi A, Jamimoghaddam M. "Fault diagnosis of a centrifugal pump using electrical signature analysis and support vector machine," J. Vib. Eng. Technol., 2023; 11(5): 2057-2067, https://doi.org/10.1007/s42417-022-00687-6.
22. Zhang Y, Wang S, Shi J, Yang X, Zhang J, Wang X. "SAR performance-based fault diagnosis for electro-hydraulic control system: A novel FDI framework for closed-loop system," Chin. J. Aeronaut., 2022; 35(10): 381-392, https://doi.org/10.1016/j.cja.2021.06.001.
23. Shanbhag VV, Meyer TJJ, Caspers LW, Schlanbusch R. "Failure monitoring and predictive maintenance of hydraulic cylinder-state-of-the-art review," IEEE-ASME Trans. Mechatron., 2021; 26(6): 3087-3103, https://doi.org/10.1109/TMECH.2021.3053173.
24. Chao Q, Gao H, Tao J, Wang Y, Zhou J, Liu C. "Adaptive decision-level fusion strategy for the fault diagnosis of axial piston pumps using multiple channels of vibration signals," Sci. China Technol. Sci., 2022; 65(2): 470-4803, https://doi.org/10.1007/s11431-021-1904-7.
25. Kosova F, Unver HO. "A digital twin framework for aircraft hydraulic systems failure detection using machine learning techniques," Proc. Inst. Mech. Eng. Part C-J. Eng. Mech. Eng. Sci., 2023; 237(7): 1563-1580, https://doi.org/10.1177/09544062221132697.
26. Pei MC, Li HR, Yu H. "Degradation state identification for hydraulic pumps using modified hierarchical decomposition and image processing," Meas. Control, 2022; 55(1-2): 21-34, https://doi.org/10.1177/00202940211064803.
27. Wang H, Wang J, Zhao Y, Liu Q, Liu M, Shen W. "Few-shot learning for fault diagnosis with a dual graph neural network," IEEE Trans. Ind. Inform., 2023; 19(2): 1559-1568, https://doi.org/10.1109/TII.2022.3205373.
28. Zou L, Lam HF, Hu J. "Adaptive resize-residual deep neural network for fault diagnosis of rotating machinery," Struct. Health Monit., 2023; 22(4): 2193-2213, https://doi.org/10.1177/14759217221122266.
29. Yan H, Sun J, Zuo H. "Anomaly detection based on multivariate data for the aircraft hydraulic system," Proc. Inst. Mech. Eng. Part I-J Syst Control Eng., 2021; 235(5): 593-605, https://doi.org/10.1177/0959651820954577.
30. Yin X, Mou Z, Wang Y. "Fault diagnosis of wind turbine gearbox based on multiscale residual features and ECA-Stacked ResNet," IEEE Sens. J., 2023; 23(7): 7320-7333, https://doi.org/10.1109/JSEN.2023.3244929.
31. Xu X, Li C, Zhang X, Zhao Y. "A dense ResNet model with RGB input mapping for cross-domain mechanical fault diagnosis," IEEE Instrum. Meas. Mag., 2023; 26(2): 40-47, https://doi.org/10.1109/MIM.2023.10083021.
32. Mishra RK, Choudhary A, Fatima S, Mohanty AR, Panigrahi BK, "A fault diagnosis approach based on 2D-vibration imaging for bearing faults," J. Vib. Eng. Technol., 2023; 11(7): 3121-3134, https://doi.org/10.1007/s42417-022-00735-1.
33. Groumpos PP. "A critical historic overview of artificial intelligence: Issues, challenges, opportunities, and threats," Artif. Intell. Appl., 2023; 1(4): 197-213, https://doi.org/10.47852/bonviewAIA3202689.
34. Xu L, Pan Z, Liang C, Lu M. "A fault diagnosis method for PV arrays based on new feature extraction and improved the fuzzy C-Mean clustering," IEEE J. Photovolt., 2022; 12(3): 833-843, https://doi.org/10.1109/JPHOTOV.2022.3151330.
35. Peng J, Kimmig A, Wang D, Niu Z, Zhi F, Wang J, Liu X, Ovtcharova J. "A systematic review of data-driven approaches to fault diagnosis and early warning," J. Intell. Manuf., 2022; 34(8): 3277-3304, https://doi.org/10.1007/s10845-022-02020-0.